Available online at www.sciencedirect.com
ScienceDirect
Developmental Biology 306 (2007) 824–837
DEVELOPMENTAL BIOLOGY
www.elsevier.com/locate/ydbio

Genomes & Developmental Control

Hau-Pax3/7A is an early marker of leech mesoderm involved in segmental morphogenesis, nephridial development, and body cavity formation

Jeffrey B. Woodruff [1], Brian J. Mitchell [2], Marty Shankland *

Section of Molecular Cell and Developmental Biology and Institute of Cellular and Molecular Biology, University of Texas at Austin, Austin, TX 78712, USA

Received for publication 28 November 2006; revised 17 February 2007; accepted 2 March 2007
Available online 12 March 2007

Abstract

Two genes of the Pax III subfamily, *Hau-Pax3/7A* and *-Pax3/7B*, were identified from the leech *Helobdella*, and the expression and function of *Hau-Pax3/7A* in development are described. Leech embryos undergo spiral cleavage, then produce a set of teloblastic stem cells that generate segmented mesoderm and ectoderm. *Hau-Pax3/7A* is present as a maternal transcript in both ectodermal and mesodermal progenitors, but this pool of early RNA disappears and is replaced by a pattern of zygotic transcription restricted to the blast cell progeny of the mesodermal M teloblasts. Each mesodermal blast cell clone goes through multiple phases of *Hau-Pax3/7A* expression, the last of which is associated with the organogenesis of the nephridia and other segment-specific structures. Morpholino-mediated knockdown of *Hau-Pax3/7A* expression causes the mesodermal blast cell clones to undergo irregular patterns of morphogenesis that disrupt the segmental organization of the germinal plate, and interferes with both the specification and morphological differentiation of the mesodermal nephridia. Knockdown of *Hau-Pax3/7A* in the mesoderm can also lead to abnormalities in the formation of the dorsal cavities, possibly through indirect effects of this germ layer on neighboring tissues. This is the first report of broad mesodermal Pax III expression outside of chordates, and raises the possibility that such expression may be a primitive trait inherited from the last common ancestor of the bilaterian superphyla.

Keywords: *Pax* gene; Leech; Mesoderm; Morphogenesis; Nephridium; Body cavity

Introduction

The spiralians are a group of bilaterian animals that includes annelids, molluscs, and several other taxa from the superphylum *Lophotrochozoa* (Passamaneck and Halanych, 2006). Spiralians are named for a highly conserved pattern of embryonic cell divisions in which the sixth cleavage gives rise to a dorsal blastomere, the 4d mesentoblast, that generates the preponderance of adult mesoderm (van den Biggelaar et al., 1997; Boyer et al., 1998; Henry and Martindale, 1998). There is a wealth of embryological data on the specification events that lead to mesentoblast formation (Freeman and Lundelius, 1992; Lambert and Nagy, 2003), but little is known at the molecular level about the differentiation of its mesodermal descendants. We here describe a *Pax* gene from the leech *Helobdella* that is prominently expressed in the descendants of the mesentoblast, and important for the morphogenesis and differentiation of the mesodermal germ layer.

The mesentoblast of leech embryos is designated as cell DM″ (Bissen and Weisblat, 1989). This blastomere cleaves symmetrically to produce a pair of large embryonic stem cells, the M teloblasts, that generate the right and left mesoderm respectively throughout the body's length (Zackson, 1982; Weisblat and Shankland, 1985). The teloblasts undergo a series of highly asymmetric stem cell divisions, producing linear columns of primary m blast cell daughters (Fig. 1A). Each m blast cell will serve as a hemisegmental founder cell of the mesoderm, and the order of blast cell birth predicts the anteroposterior (AP) position of blast cell clones in the mature leech (Fig. 1B). In contrast to the majority of spiralians, the ectoderm of the leech is also produced by large, teloblastic stem

* Corresponding author. Fax: +1 512 471 3878.
E-mail address: hastypig@mail.utexas.edu (M. Shankland).
[1] Present address: Graduate Program in Molecular and Cell Biology, University of California, Berkeley, CA 94720, USA.
[2] Present address: Molecular Neurobiology Laboratory, Salk Institute, 10010 North Torrey Pines Road, La Jolla, CA 92037, USA.

0012-1606/$ - see front matter © 2007 Elsevier Inc. All rights reserved.
doi:10.1016/j.ydbio.2007.03.002

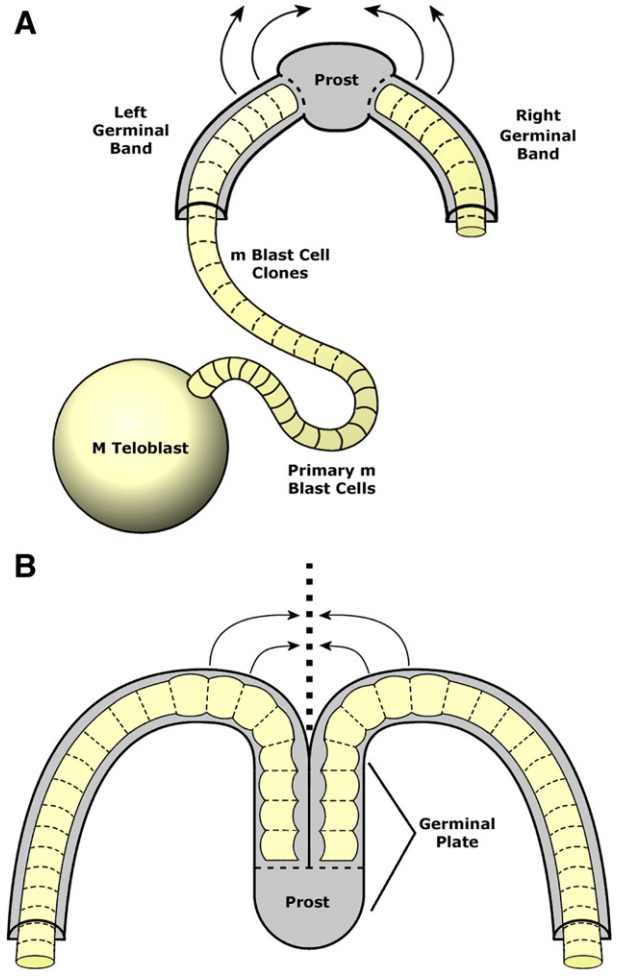

Fig. 1. Formation of segmental mesoderm in leech. (A) Mesoderm (yellow) arises from a bilateral pair of M teloblasts. Each teloblast undergoes repeated stem cell divisions to produce a linear column of primary m blast cell daughters, which divide to form clones as they mature. The oldest clones lie furthest from the teloblast, and are attached to the prostomium (prost). Each column of mesoderm comes to lie under an arched layer of ipsilateral ectoderm – portrayed as transparent – to form a germinal band (grey). As they lengthen, the right and left bands move symmetrically over the surface of the embryo (arrows). (B) During embryonic stage 8, the right and left germinal bands meet and fuse along the ventral midline (dashed line) to form the germinal plate. The anterior end of the plate is the unsegmented prostomium. The firstborn m blast cells contribute mesoderm to the anteriormost segments.

cells that divide in a manner overtly similar to the M teloblast (Weisblat and Shankland, 1985).

The M teloblast lineage merges with the four ipsilateral ectodermal teloblast lineages to form a bilayered germinal band. Merger begins with the anteriormost – i.e., firstborn – blast cells, and moves posteriorly as successively younger blast cells are incorporated into the band (Fig. 1). The time-course of blast cell maturation can be reconstructed within a given teloblast lineage from the posterior-to-anterior sequence of blast cell clones (Zackson, 1982, 1984). During gastrulation, the elongating germinal bands slide over the surface of the embryo until they meet along the future ventral midline to form a germinal plate (Fig. 1). The plate undergoes organogenesis to produce the tissues of the adult leech, and is subdivided into four domains: an unsegmented head domain or prostomium; four rostral segments (R1–4); twenty-one midbody segments (M1–21); and seven caudal segments (C1–7).

Experimental studies suggest that the mesodermal fate of the M teloblasts is specified by factors already present in the uncleaved zygote (Nelson and Weisblat, 1992). However, the molecular basis of mesoderm development is unclear, since the only described gene products that are expressed in the teloblasts and/or primary blast cells of the leech embryo are distributed in all five lineages (Goldstein et al., 2001; Song et al., 2002, 2004; Rivera et al., 2005). Mesoderm-specific gene expression has been reported in certain other spiralian embryos (Yang and Collier, 1993; Hinman and Degnan, 2002), but *Pax* genes have not been implicated to date.

The *Pax* genes encode a family of transcription factors that is conserved across metazoan animals (Miller et al., 2000; Matus et al., 2007). The ancestral *Pax* gene is thought to have had at least two separate DNA-binding motifs: an upstream paired domain and a downstream homeodomain. However, part or all of the homeodomain has been deleted in certain subfamilies (Balczarek et al., 1997), and partial deletions of the paired domain have also occurred (Hobert and Ruvkun, 1999). In bilaterian animals, *Pax* genes are generally subdivided into four or five major groups on the basis of sequence similarity and domain organization, and we will here refer to Pax Groups I–IV as defined by Balczarek et al. (1997). The bilaterian *Pax III* genes – also known as *Pax3/7* – show a close affinity to the *PaxD* genes of anthozoans, suggesting that this subfamily diverged from Pax Groups I, II, and IV prior to the separation of Bilateria and Cnidaria (Matus et al., 2007).

In bilaterian animals, *Pax III* genes have been extensively studied in arthropods (superphylum *Ecdysozoa*) and chordates (superphylum *Deuterostomia*), but not the superphylum *Lophotrochozoa*. During *Drosophila* development, the *Pax III* genes *paired* (*prd*) and *gooseberry* (*gb*) initially function in the segmentation of the germ band, and later become involved with paralog *gooseberry-neuro* in various aspects of neurogenesis (Noll, 1993). This dual role in segmentation and neurogenesis is widespread among the arthropods, including short germ band insects, myriapods, crustaceans, and chelicerates (Davis et al., 2001, 2005; Dearden et al., 2002; Schoppmeier and Damen, 2005). Mesodermal expression of *Pax III* genes has been reported in arthropods, but is a minor component of the expression pattern (Gutjahr et al., 1993; Davis et al., 2005).

The *Pax III* genes of vertebrate chordates are *Pax3* and *Pax7*. These two genes are involved in neural patterning, e.g., the specification of neural crest (Goulding et al., 1991; Mansouri et al., 1996), and orthologs in other chordates are likewise expressed in the dorsal neuroectoderm (Wada et al., 1997; Holland et al., 1999). In addition, *Pax3* and *Pax7* are widely expressed in the somites of vertebrate embryos, where they play distinct roles in muscle development (Goulding et al., 1994; Oustanina et al., 2004). The *AmphiPax3/7* gene of cephalochordates is also expressed in somitic mesoderm (Holland et al., 1999), but orthologs in urochordates do not

show mesodermal expression (Wada et al., 1997; Mazet et al., 2003). Unlike their arthropod homologues, the chordate *Pax III* genes have not been implicated in the process of body axis segmentation.

We here report the identification of two lophotrochozoan *Pax III* genes, and describe the developmental expression and function of one gene in detail. *Hau-Pax3/7A* is an early molecular marker of the mesentoblast-derived mesoderm of the leech embryo, showing intense zygotic expression in the blast cells produced by the M teloblasts. Morpholino knockdown experiments indicate that *Hau-Pax3/7A* plays important roles in segmental morphogenesis, the development of the nephridia, and body cavity formation.

Materials and methods

Animals

Embryos were taken from a laboratory breeding colony of *Helobdella* leeches collected in Austin, Texas. These leeches were originally described as *Helobdella robusta* on the basis of morphology (Seaver and Shankland, 2000), but molecular phylogenetic analysis (Bely and Weisblat, 2006) reveals that they are a distinct and as yet unnamed species, here referred to as *Helobdella* sp. (Austin).

Postembryonic leeches were maintained in 1% artificial seawater, and fed thrice weekly on pond snails collected at U. Texas Brackenridge Field Laboratory. Embryos were raised at 24 °C in a defined saline, and staged according to the Stent et al. (1992) system for *Helobdella triserialis*.

Molecular characterization

Hau-Pax3/7A and *-Pax3/7B* were initially isolated from leech embryo cDNA by the polymerase chain reaction (PCR) using degenerate primers. *Hau-Pax3/7A* was amplified with primers targeted to conserved amino acid sequences in the paired domain (KIVEMA) and homeodomain (YPDIYT). *Hau-Pax3/7B* was isolated with primers targeted to two other conserved sequences in the paired domain (VSHGCV and QETGSI). Primer sequences are available on request.

The FirstChoice RLM-RACE kit (Ambion) was employed to extend these sequences in the 5′ and 3′ directions using gene-specific primers. For *Hau-Pax3/7A*, overlapping 5′- and 3′-RACE products were ligated at an *Xho*I site (Nt 908–913) to generate a full-length cDNA.

The phylogenetic relationships of *Hau-Pax3/7A* and *-Pax3/7B* were examined with PAUP (4.0b10).

Reverse transcription PCR (RT-PCR)

Accumulation of *Hau-Pax3/7A* RNA was investigated by RT-PCR. Embryonic RNA was extracted with the RNAqueous kit (Ambion), and reverse-transcribed with random primers. For each developmental stage, two separate regions of the *Hau-Pax3/7A* transcript (Nt 373–611 and Nt 1300–1533) were amplified using gene-specific primers. An 18S rRNA sequence was amplified in parallel as a loading control (QuantumRNA, Ambion).

In situ hybridization

The cellular distribution of RNA was characterized by the whole-mount *in situ* hybridization method of Nardelli-Haefliger and Shankland (1992) with digoxigenin–labeled sense and antisense riboprobes generated from the complete *Hau-Pax3/7A* cDNA. Hybridization was visualized by alkaline phosphatase immunostaining using the NBT and BCIP substrates. Stained embryos were either cleared in glycerol, or dehydrated and cleared in a 3:2 mixture of benzyl benzoate:benzyl alcohol. Some specimens were embedded in POLYBed 812 plastic (Polysciences) and handcut by razor blade into 0.1-mm sections. Specimens were imaged with a Diagnostic Instruments Spot CCD camera.

Morpholino injections

Carboxyfluorescein-tagged morpholino oligomers (MOs) were synthesized by Gene Tools, LLC. The antisense sequence MO1 (CATTTCTAA-GAATTTGCTTGTTCAT) is complementary to the first 25 nucleotides of the *Hau-Pax3/7A* coding sequence; antisense sequence MO2 (CAT-GATGGTGTTTTCCAACGAGTAT) is complementary to the last 22 nucleotides of 5′-UTR and the predicted initiation codon. Both antisense MOs show < 60% complementarity to the *Hau-Pax3/7B* transcript, and should not effect its expression. Control MOs employed here include the manufacturer's 'standard' control sequence and a 'mismatch' control derived from the MO2 sequence: CATCATCGTGTTTTGCAACCACTAT (mismatched bases underlined).

Zygotes and blastomeres were microinjected with a 2:1 mixture of 1.0 mM MO to 4% fast green FCF, with the fast green being used to monitor injection volume. For each target cell we identified a volume of manufacturer's control MO that did not perturb development, and used comparable volumes of MO1, MO2, and the mismatch control. The intracellular MO concentration used in these experiments was calculated to be roughly 1 μM.

Lineage tracing

To trace individual cell lineages, identified blastomeres were microinjected with 10 kDa tetramethylrhodamine or biotin dextran-amine (Molecular Probes). Biotin-labeled embryos were permeabilized, blocked with 10% normal goat serum, and stained with an avidin/horseradish peroxidase complex (ABC Kit; Vector) using diaminobenzidine as substrate. Labeled embryos were examined on a Nikon E800 fluorescence microscope, and some optically sectioned with a Zeiss LSM5 Pascal confocal microscope.

Results

Molecular characterization

Two novel *Pax III* gene products were isolated from cDNA of *Helobdella* sp. (Austin) by degenerate PCR, and designated as *Hau-Pax3/7A* and *-Pax3/7B*. Comparison with the whole genome sequence project of the closely related species *H. robusta* (NCBI) indicates that these sequences derive from separate genes. The present paper characterizes *Hau-Pax3/7A*; the second gene will be described in detail in a later publication.

A 1906 bp *Hau-Pax3/7A* cDNA was constructed from overlapping 5′- and 3′-RACE products. This sequence has an open-reading frame (ORF) that starts with the first ATG that encodes a 472-amino-acid polypeptide containing both paired domain and homeodomain motifs (Fig. 2). The majority of known *Pax III* genes also have a conserved octapeptide sequence between the paired domain and homeodomain (Balczarek et al., 1997), but there is no obvious counterpart of this octapeptide in the *Hau-Pax3/7A* gene product. The 3′-UTR contains a polyadenylation signal sequence (Nt 1893–1898) immediately preceding the poly-A tail.

Phylogenetic analysis of both the paired domain and homeodomain indicates that these two leech genes are members of the Pax III subfamily (Fig. 3). Previous work has suggested that the last common ancestor of bilaterian animals had a single *Pax III* gene (Balczarek et al., 1997; Matus et al., 2007), and our findings are generally consistent with that idea. The paired domains of *Hau-Pax3/7A* and *-Pax3/7B* show closer affinity to one another (68% of bootstrap replicates) than to a selection of *Pax III* genes from chordates and arthropods (Fig. 3A). The two

Fig. 2. Sequence comparison of the paired domain (A) and homeodomain (B) between *Hau-Pax3/7A* and the *Pax III* genes of fly and mouse. Conserved amino acids are boxed in black.

leech genes also show a strong affinity to the Pax III group in terms of homeodomain sequence, but the *Hau-Pax3/7B* homeodomain is more highly diverged and sorts to a basal position within this group (Fig. 3B).

The consensus *Hau-Pax3/7A* cDNA sequence has been deposited under GenBank accession no. DQ858213, and a partial *Hau-Pax3/7B* sequence has been deposited under GenBank accession no. EF133692.

Developmental time-course

The time-course of *Hau-Pax3/7A* RNA expression was examined by RT-PCR using primer pairs flanking known splice sites (Fig. 4). RNA was detected in oocytes and uncleaved zygotes, indicating that *Hau-Pax3/7A* is initially present in development as a maternal transcript. The level of *Hau-Pax3/7A* RNA remains relatively constant through the first 10 days of embryonic development. We expect that maternal RNA is replaced by zygotic transcripts during this time, but that transition was not readily apparent in the overall profile of RNA accumulation (Fig. 4). Hence, there is likely to be a developmental interval during which the embryo contains both the maternal and zygotic RNA.

In situ hybridization

The cellular distribution of *Hau-Pax3/7A* RNA was characterized by *in situ* hybridization with digoxigenin-labeled antisense riboprobes. Control hybridizations with sense probes gave little or no staining at the stages examined.

Zygote and cleavage stages

Following zygote deposition, the cytoplasm of the *Helobdella* embryo undergoes reorganization to form two pools of RNA-rich 'teloplasm' situated beneath the animal and vegetal poles (Holton et al., 1994). *Hau-Pax3/7A* RNA is primarily localized to the teloplasm, although we detected some hybridization in the perinuclear cytoplasm as well (Fig. 5A). During the cleavage divisions of early embryogenesis, the teloplasm and its *Hau-Pax3/7A* transcripts are subdivided among the ten teloblastic stem cells (Figs. 5B, C). This subdivision appears to be uniform, i.e., we did not observe differences in the intensity of staining between the various teloblasts or their progenitors at any stage. *Hau-Pax3/7A* RNA is also detected in the micromere cap at stages 5–6 (Fig. 5B), possibly through an inheritance of the perinuclear transcripts seen at earlier stages.

The level of *Hau-Pax3/7A* RNA within the teloblasts diminishes during embryonic stage 6, and ceases to be detectable with *in situ* hybridization by the middle of stage 7 (Figs. 5C–E). There is an onset of intense *Hau-Pax3/7A* expression in the blast cells of the M teloblast lineage during those stages, indicating that the loss of teloblast staining is not a histological artifact and likely results from RNA degradation.

Teloblast lineages

Starting with blast cell formation, expression of *Hau-Pax3/7A* is almost entirely restricted to the mesodermal descendants of the M teloblast. RNA expression was observed in the primary, undivided m blast cells (Fig. 5C). In sectioned specimens, it was often possible to observe hybridization in that blast cell produced by the most recent teloblast division (Figs. 5D, E). Given the absence of detectable staining in the parent teloblast, this observation suggests that nascent m blast cells initiate zygotic transcription of *Hau-Pax3/7A* in the 1.5-h interval before the next m blast cell is born. In contrast, no *Hau-Pax3/7A* expression was observed at any stage in the blast cell progeny or differentiated descendants of ectodermal teloblasts.

Each of the two M teloblasts produces a column of greater than thirty m blast cell daughters, which enter the posterior end of the ipsilateral germinal band and travel through it to the germinal plate (Fig. 1). These blast cell columns express *Hau-Pax3/7A* as they depart from the right and left teloblasts (Fig. 5C), but that expression is transient and the RNA disappears before the m blast clones enter the germinal band (Fig. 6A).

Hau-Pax3/7A expression resumes at specific positions within the germinal band, corresponding to specific stages of blast cell maturation. The second phase of blast cell expression occurs when the m blast cell clone has traveled 6–8 clonal

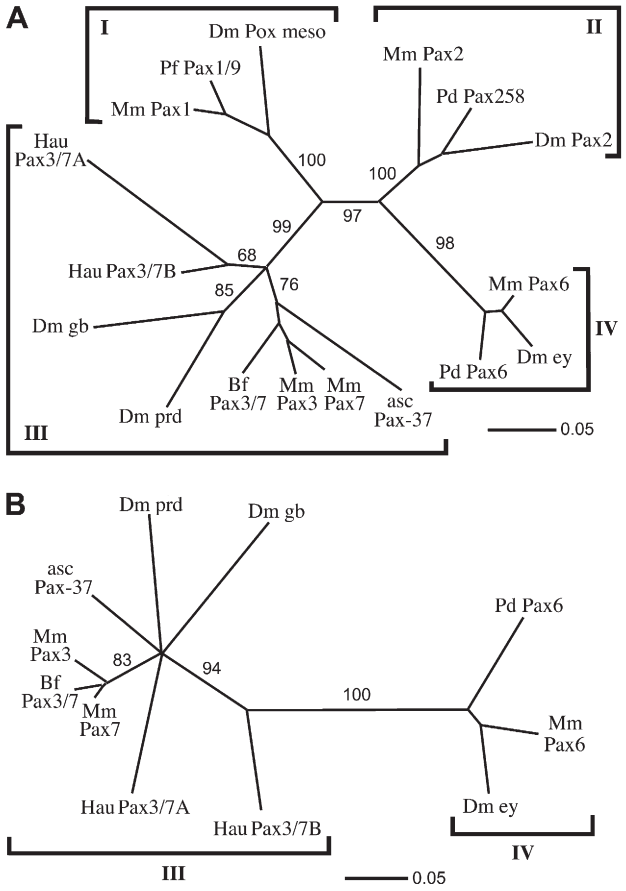

Fig. 3. *Hau-Pax3/7A* and *-Pax3/7B* show an affinity to *Pax III* genes of deuterostomes and ecdysozoans in phylogenetic analyses of paired domain (A) and homeodomain (B) protein sequence. Only *Pax* Group III and IV genes have complete homeodomains (Balczarek et al., 1997) and are included in part B. Unrooted phylograms were generated by neighbor-joining distance analysis, and numbers represent bootstrap percentages from 1000 replicates. Branches with values less than 50% have been collapsed, and some bootstrap values are left out for simplicity. Sequences taken from: *Drosophila melanogaster (Dm) prd* [GenBank accession no. P06601]; *Dm gsb* [P09082]; *Dm ey* [I45557]; *Dm Pax2* [NP_524633]; *Dm Pox meso* [NM_079552]; *Mus musculus* (*Mm*) *Pax3* [AAH48699]; *Mm Pax7* [AAG16663]; *Mm Pax1* [AAK01146]; *Mm Pax2* [P32114]; *Mm Pax 6* [AAH11272]; *Branchiostoma floridae (Bf) Pax3/7* [AAF89581]; *Halocynthia roretzi (asc) Pax-37* [BAA12289]; *Platynereis dumerilii* (*Pd*) *Pax258* [CAD43608]; *Pd Pax6* [CAJ40659]; *Ptychodera flava (Pf) Pax1/9* [ABO20763].

lengths into the band (Fig. 6A). The primary blast cell is undergoing its third round of cell divisions at this time, and *Hau-Pax3/7A* expression is restricted to a subset of cells on the clone's future ventral edge (Figs. 6B, C). The second phase of expression is brief. At a given developmental time point, this particular staining pattern is restricted to a stretch of 1–3 consecutive m blast cell clones (Fig. 6), indicating that the RNA accumulates and is then degraded within a 2- to 5-h interval of blast cell maturation.

Organogenesis

The tertiary phase of *Hau-Pax3/7A* expression in blast cells varies in accordance with the segmental identity of the m blast cell clone. In some segments the pattern of tertiary expression is closely linked to nephridial development. Nephridia are conventionally designated by the segmental location of their excretory pores (Weisblat and Shankland, 1985), which in *Helobdella* are located in two midbody domains: segments M2–5 and M8–18 (Fig. 7G).

As they approach the germinal plate, those m blast cell clones that are destined to produce nephridia begin to express *Hau-Pax3/7A* in a single large cell, as well as 1–2 smaller cells that are located nearer the ventral midline (Figs. 7A–C). The fate of the small cell(s) is unknown. The large cell appears to be the 'nephridioblast' described by Bürger (1891), and divides repeatedly during stages 8–9 to produce the nephridial tissue. The developing nephridia express *Hau-Pax3/7A* throughout the time-course of their differentiation, including the latest stages examined (Figs. 7G, H). Lineage tracer analysis indicates that *Hau-Pax3/7A* expression is restricted to the mesodermal portion of the nephridium, and does not extend to the ectodermal cells of the distal tubule or nephridiopore (Shankland and Weisblat, 1984).

Midbody segments M6 and M7 do not develop nephridia (Weisblat and Shankland, 1985), and we never observed intensely staining nephridioblasts in the m blast cell clones destined for those segments. However, we encountered several embryos with what appeared to be faint, transient expression of *Hau-Pax3/7A* in an M6 or M7 nephridioblast (Fig. 7B). One interpretation is that these segments generate a lineal homologue of the nephridioblast, but that cell aborts nephridial development at this early stage. Segments M6 and M7 also contain the small ventral cell(s), whose *Hau-Pax3/7A* expression level is comparable to that seen in adjacent segments (Fig. 7B).

We saw a distinct pattern of tertiary *Hau-Pax3/7A* expression in four more anterior m blast cell clones that do not produce nephridia (Figs. 7A–C). A mature m blast cell clone is distributed across three consecutive segments (Weisblat and Shankland, 1985), which complicates the naming of clones on the basis of segmental location. This alternative *Hau-Pax3/7A* expression pattern was observed in those m clones whose posterior boundary – the site of any associated nephridiopore – will come to lie in rostral segments R2–4 and midbody segment M1 of the mature body plan. These particular clones express *Hau-Pax3/7A* as they enter the germinal plate (Fig. 7A), and as development proceeds the expressing cells form obliquely

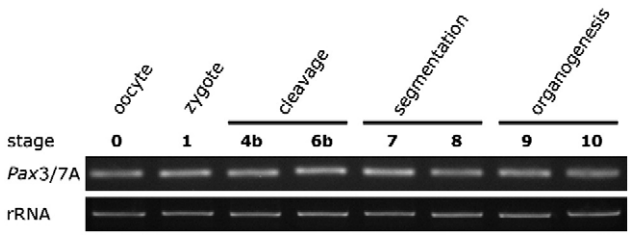

Fig. 4. RT-PCR reveals maternal *Hau-Pax3/7A* RNA in oocyte and zygote, and a relatively constant level of expression over a 10-day period of embryogenesis. Similar results were obtained with a second downstream primer pair (not shown). Sample loading was normalized by amplification of 18 S rRNA.

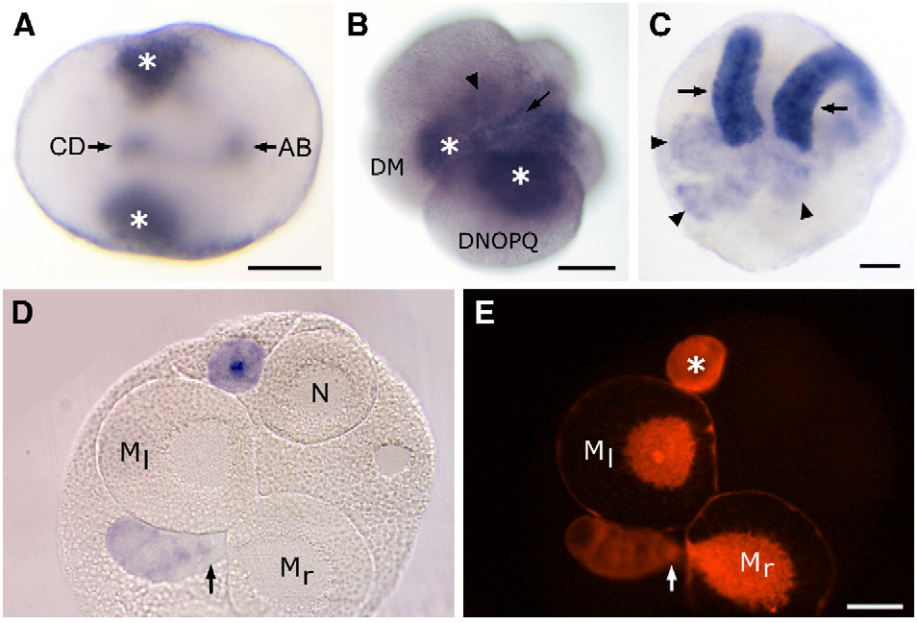

Fig. 5. Early *Hau-Pax3/7A* expression seen by *in situ* hybridization. (A) Side view of zygote in telophase. *Hau-Pax3/7A* RNA occurs predominantly in two pools of teloplasm (asterisks), and is also visible in perinuclear cytoplasm (arrows) being segregated to daughter cells AB and CD. (B) Animal pole view at stage 4c. Teloplasmic *Hau-Pax3/7A* RNA (asterisks) has been divided between ectodermal progenitor DNOPQ and mesodermal progenitor DM. Fainter staining is visible in micromeres (arrow) and perinuclear cytoplasm of a macromere (arrowhead). (C) Animal view of stage 7 embryo, D quadrant at bottom. All of the m blast cells express *Hau-Pax3/7A* at this stage, and they are arrayed in bilateral columns (arrows) extending from the right and left teloblasts towards the future sites of germinal band formation. Residual staining of ectodermal and mesodermal teloblasts is faint (arrowheads). (D, E) Section of older stage 7 embryo viewed with Nomarski optics (D) and fluorescence (E). Both M teloblasts were injected with rhodamine dextran prior to blast cell formation. Blast cell daughters of the M_r teloblast, including the most recent (arrow), show *Hau-Pax3/7A* expression. Blast cells from the M_l teloblast, seen in cross-section (asterisk), also express *Hau-Pax3/7A*. Scale bars: 100 μm in panels A–C; 50 μm in panels D–E.

oriented bars that converge on the ventral midline (Fig. 7C). The bar-shaped structures shift posteriorly during later stage 8 (Fig. 7C), and are eventually displaced 4–5 segments from their segments of origin. They cease to express *Hau-Pax3/7A* during stage 9, a time when we could not yet assign a definitive fate. Lineage tracing indicates that the bars are composed of mesodermal cells lying immediately adjacent to the midgut primordium (Figs. 7D, E), suggesting that this cell population may become part of the anterior midgut (Nardelli-Haefliger and Shankland, 1993).

We did not observe a tertiary phase of *Hau-Pax3/7A* expression in the ten most posterior segments (M19-C7) of the *Helobdella* germinal plate. These segments fail to produce nephridia.

Prostomium

Although *Hau-Pax3/7A* expression is restricted to the mesodermal M lineage in the segmented portion of the body, in a subset of embryos we also observed 1–2 *Hau-Pax3/7A*-expressing cells in the ectoderm of the prostomium, an unsegmented head domain at the anterior end of the germinal plate (Fig. 1). This staining pattern was only seen around the stage 7 to stage 8 transition, and was located asymmetrically in the right anterior prostomial quadrant (Fig. 7F) in all 10 embryos in which it was observed. Lineage tracer injections revealed that the expressing cells do not derive from the M teloblast, and are therefore likely to originate from one of the embryonic micromeres (Smith and Weisblat, 1994).

Morpholino injections

To ascertain the developmental function of *Hau-Pax3/7A*, we injected both zygotes and later stage embryos with antisense MOs directed to its translation start site. MO1 and MO2 gave similar developmental phenotypes, but MO2 generally had a stronger effect and was used for the majority of experiments. Antisense injections were performed in parallel with injections of either the manufacturer's standard control or a custom mismatch control sequence (see Materials and methods). Both control MOs had little or no effect on development, and the results obtained with the two controls have been summed.

Antisense MOs can act by chance hybridization to knock-down the expression of other, untargeted gene products that would not hybridize with control MOs. To control for this possibility we injected MO1 and MO2 into ectodermal teloblasts, whose descendants do not express *Hau-Pax3/7A* (see above). Neither antisense morpholino had any effect on the highly stereotyped patterns of ectodermal morphogenesis (Fig. 8), suggesting that they do not disrupt the expression of other, untargeted gene products that are essential for normal teloblast development.

Zygote and mesentoblast injections

There were clearcut differences in the development of zygotes injected with antisense and control MOs. Some injected zygotes either failed to cleave or underwent abnormal cleavage soon after injection, but such abnormalities were observed with both antisense (21%) and control (12%) sequences and not

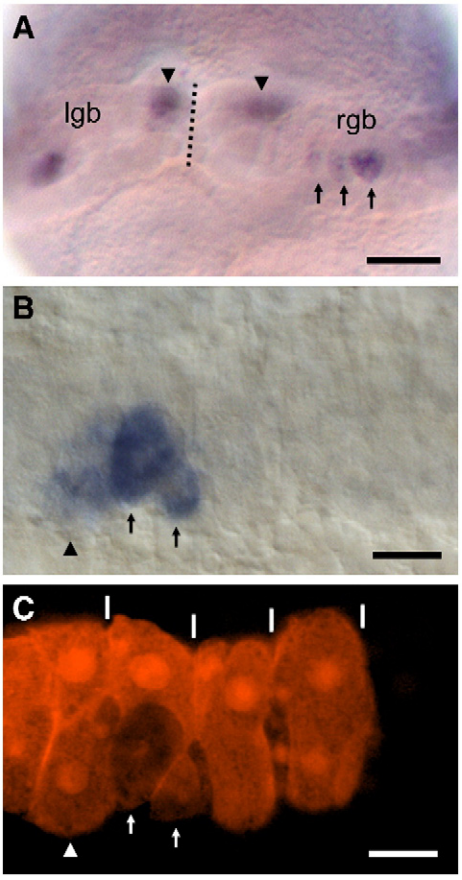

Fig. 6. The m blast cell clones experience a second brief period of *Hau-Pax3/7A* expression after entering the germinal band. (A) At stage 8 the right and left germinal bands (rgb; lgb) emerge onto the surface of embryo at the dorsal midline (dotted line), then separate and extend laterally. The right germinal band is in focus, and *Hau-Pax3/7A* RNA is visible in three consecutive m blast cell clones (arrows). Primary blast cell expression can also be seen deep within embryo (arrowheads). (B, C) Germinal band in which the M lineage was labeled with rhodamine dextran, and viewed by Nomarski optics (B) and confocal fluorescence microscopy (C). Anterior is to the right; future dorsal towards the top. Primary m blast cell clones have undergone 2–3 rounds of cell division, and are demarcated by white bars. *Hau-Pax3/7A* is expressed intensely in two cells (arrows) located on the ventral side of one clone. A fainter level of expression is seen in one or more cells (arrowhead) in the next posterior clone. Certain other cells show less intense fluorescence, but contain no apparent reaction product. Scale bars: 50 μm in panel A; 10 μm in panels B–C.

studied further. Among those zygotes that underwent normal cleavage, 87% (39/45) of the MO2-injected embryos developed gross abnormalities during stage 8 and died without hatching from the vitelline envelope. Consistent defects included a delay in formation of the dorsal body cavities and morphological collapse of the midgut primordium (see below). Zygotes injected with either control MO never showed these defects, with 92% (109/118) hatching at stage 9 and developing normally for 2–4 days thereafter.

Given that later *Hau-Pax3/7A* expression is primarily in the mesoderm, we compared the effect of injecting antisense MOs into mesodermal progenitor DM″. The fluorescein-tagged MOs remain sequestered in the injected cell lineage, suggesting that they cannot have a direct effect on gene expression in other lineages. When cell DM″ was injected with MO2, 98% (134/137) of embryos developed a suite of morphological abnormalities indistinguishable from that seen with zygote injections (Figs. 9C and 10C, D). In contrast, development was normal

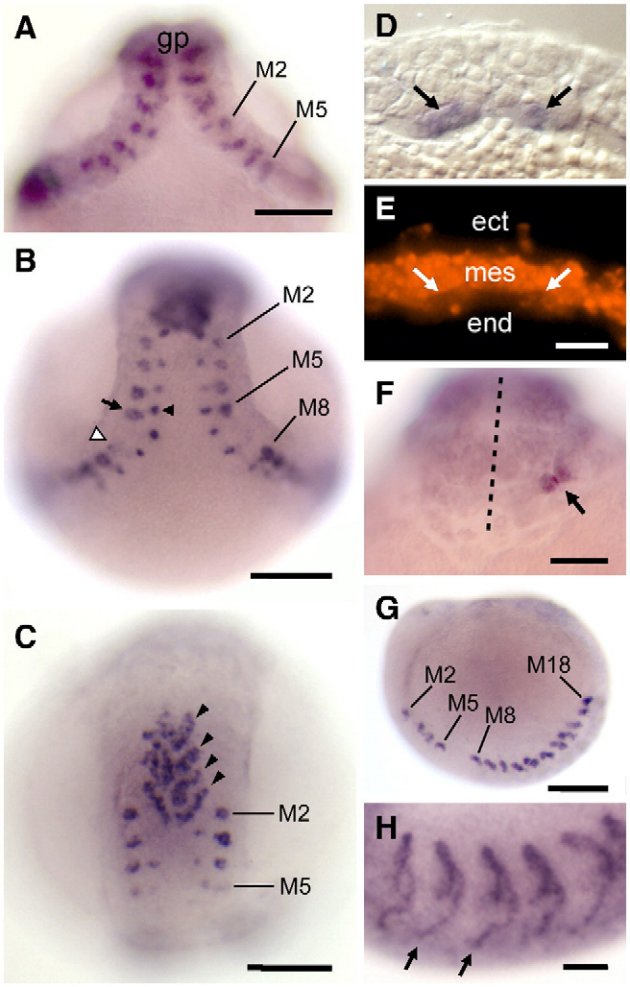

Fig. 7. *Hau-Pax3/7A* expression in the germinal plate. Nephridia and their progenitor cells are numbered according to segment. (A–C) Stage 8 embryos at three sequential times in development, in ventral view with anterior to the top. In panel A, the segmentally organized m blast cell clones experience their third phase of *Hau-Pax3/7A* expression as they enter the germinal plate (gp). In a slightly older embryo (B), individual clones manifest a segment-specific pattern of expression. Segments that will generate nephridia show *Hau-Pax3/7A* expression in a large nephridioblast (arrow) and 1–2 smaller medial cell(s) (arrowhead). Segments M6 and M7 show intense staining of the small cell(s), and faint transient staining of a cell resembling a nephridioblast (hollow arrowhead). In panel C, four extreme anterior segments express *Hau-Pax3/7A* in oblique bar-shaped structures (arrowheads). The latter structures will be displaced posteriorly, and have encroached on segment M2 at this time. (D, E) Parasagittal section of two of the bar-shaped structures seen in part C, viewed by Nomarski optics (D) and rhodamine fluorescence (E). Ventral is to the top. These *Hau-Pax3/7A*-expressing cells (arrows) are part of the rhodamine-labeled mesoderm (mes), and lie at the interface with the yolky endoderm (end). Ectoderm (ect) is unlabeled. (F) D quadrant view of late stage 7 prostomium, with midline marked. There is asymmetric expression of *Hau-Pax3/7A* in two cells (arrowhead) on the right. (G, H) Side views of nephridial *Hau-Pax3/7A* expression. Anterior to the left; dorsal to the top. By stage 9 (G) *Hau-Pax3/7A* expression is restricted to differentiating nephridia. By stage 10 (H), each nephridium has differentiated into a coiled tubule that projects ventrally (arrows) towards the nephridiopore. Scale bars: 100 μm in panels A–C, G; 50 μm in panels F, H; 10 μm in panels D–E.

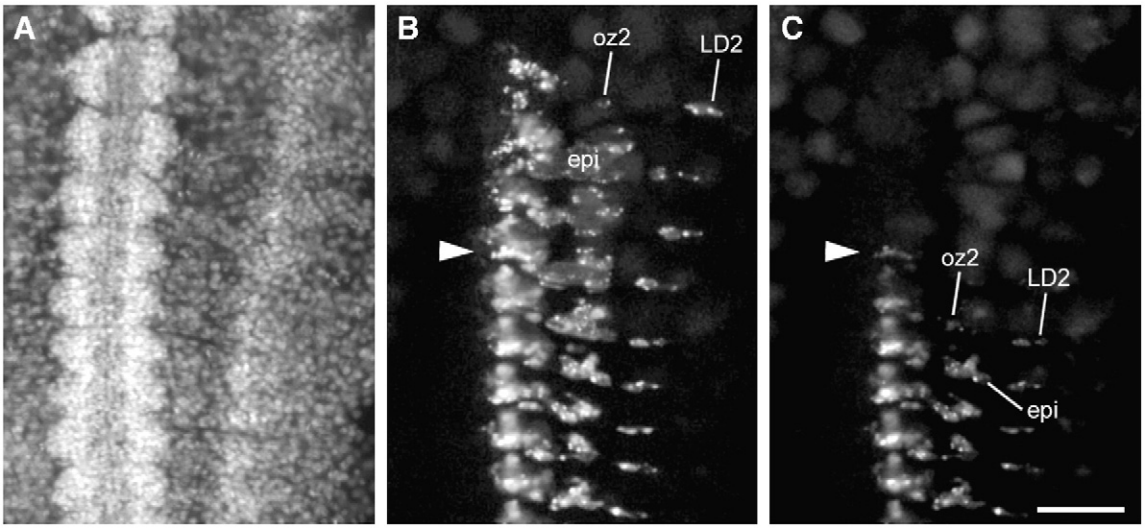

Fig. 8. *Hau-Pax3/7A* antisense MOs do not alter the development of ectodermal teloblast lineages, which do not express this gene. Images are taken from the dissected body wall of a stage 10 embryo in which the right O teloblast was injected with rhodamine–dextran at stage 7, and reinjected 4 h later with fluorescein-tagged MO2. Anterior is to the top. (A) Hoechst fluorescence showing the distribution of nuclei and gross outline of the segmental ganglia in the ventral nerve cord. (B, C) Lineage tracer fluorescence shows the descendants of the right O teloblast, including segmentally repeated clusters of central neurons, identified peripheral neurons (oz2 and LD2), and patches of epidermis (epi) characteristic for this cell lineage (Shankland and Weisblat, 1984). Panel B shows the distribution of rhodamine lineage tracer, and panel C the distribution of fluorescein tagged-MO2. The anteriormost MO2-containing clone is labeled faintly. Blast cell clones which received MO2 (below arrowhead) show the same pattern of morphogenesis as blast cell clones which did not (above arrowhead). Scale bar: 50 μm.

(Figs. 9B and 10A, B) in all embryos ($n=83$) in which cell DM″ was injected with either of the control MOs. This result suggests that *Hau-Pax3/7A* plays an important role in mesoderm development, and argues that the phenotypes produced by MO2 injection of zygotes are due in large part to *Hau-Pax3/7A* knockdown in the mesoderm. In keeping with this idea, when MO2 was injected into cell DNOPQ‴ – progenitor of the ten ectodermal teloblasts – most embryos (88%, 46/52) hatched and developed normally for 2–4 days thereafter.

Injection of MO2 into either the zygote or cell DM″ yielded a reproducible phenotype. The injected embryos developed normally for 4–5 days, during which time the teloblasts divided to produce blast cells and the blast cells assembled into germinal bands. The contour of the germinal bands was sometimes irregular, but they always began to fuse to form a germinal plate. In normal development, an extraembryonic membrane – the provisional integument – separates from the underlying midgut primordium on either side of the germinal plate to produce a bilateral pair of fluid-filled dorsal cavities (Figs. 9A, B), which are distinct from the coelomic cavities inside the germinal plate (Nardelli-Haefliger and Shankland, 1993). This separation was delayed by 1 day in MO2-injected embryos (Fig. 9C), and when the cavities did form they rapidly overinflated to produce large concave indentations in the midgut primordium (Fig. 10C). The shrinking midgut pulled free from the germinal plate in nearly all cases, eventually collapsing upon the remnants of the teloblasts (Fig. 10D). Embryos that experience midgut collapse die without hatching.

A minority of MO2-injected embryos (13%; 28/213) formed a third, anomalous fluid-filled cavity beneath the anterior end of the germinal plate. This additional cavity fused with the dorsal body cavities prior to midgut collapse.

M teloblast injections

Simultaneous injection of MO2 into the right and left M teloblasts yielded a phenotype indistinguishable from that produced by injections of the parent blastomere DM″. However, injection of a single M teloblast yielded a less severe phenotype: 95% (355/372) of those embryos hatched; and many developed for 2–4 days thereafter. The prolonged survival of these unilaterally injected embryos permitted us to

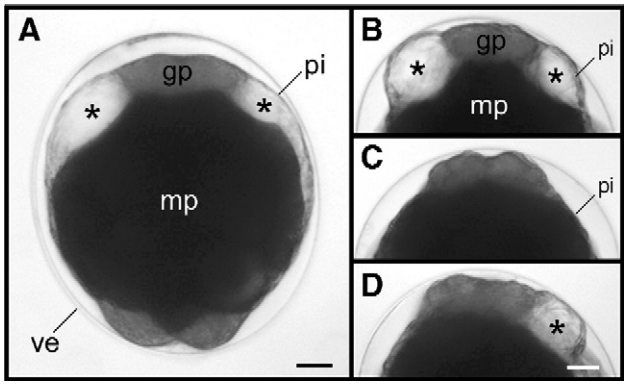

Fig. 9. *Hau-Pax3/7A* knockdown delays body cavity formation. Embryos are still enclosed in the vitelline envelope (ve), and viewed from dorsal side with anterior to the top. (A) At the onset of stage 9, the midgut primordium (mp) is encircled by the germinal plate, with the anterior end marked (gp). Dorsal body cavities (asterisks) have formed by separation of provisional integument (pi) from underlying midgut. (B–D) MO-injected stage 8 embryos from a single clutch of eggs. In panel B, cell DM″ was injected with control MO and the body cavities (asterisks) have formed normally. In panel C, cell DM″ was injected with *Hau-Pax3/7A* antisense MO. Cavity formation is delayed bilaterally. In panel D, the left M teloblast was injected with *Hau-Pax3/7A* antisense MO. Cavity formation is delayed on left, but has occurred normally on right (asterisk). Scale bars: 50 μm.

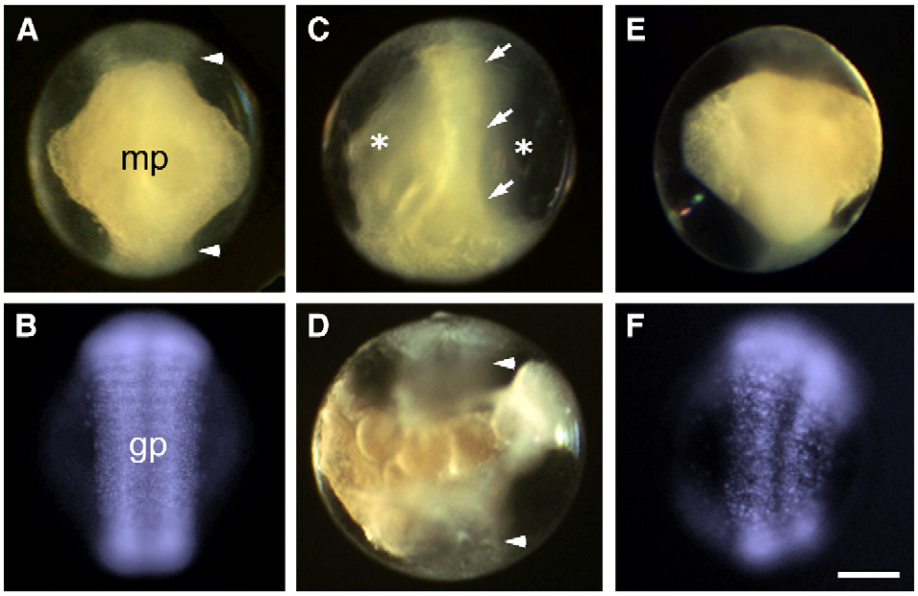

Fig. 10. *Hau-Pax3/7A* knockdown in the mesoderm causes midgut collapse. Unhatched embryos are shown from the ventral side with anterior to the top. (A, B) Normally developing stage 9 embryo in which cell DM″ was injected with control MO. Body cavities bracket the diamond-shaped midgut primordium (mp), which is encircled by the germinal plate (arrowheads). Hoechst fluorescence (B) reveals a segmentally organized pattern of nuclei in the plate (gp). (C, D) Embryos in which cell DM″ was injected with *Hau-Pax3/7A* antisense MO. In panel C, the body cavities of a stage 8 embryo have overexpanded and form concave indentations (asterisks) in the midgut, which still maintains a narrow band of contact (arrows) with germinal plate. Part D shows a comparable embryo 1 day later. Development has ceased, and the midgut has pulled away from both anterior and posterior ends of the germinal plate (arrowheads). (E, F). Embryo in which the left M teloblast was injected with *Hau-Pax3/7A* antisense MO. The midgut primordium has developed its normal diamond-shaped profile, but is displaced to the side of injection. Hoechst fluorescence (F) shows that the germinal plate also curves towards injected side. Scale bar: 100 μm.

study the effects of *Hau-Pax3/7A* knockdown on later stages of embryonic development.

Injection of MO2 into a single M teloblast affected the development of the dorsal body cavities, but the phenotype was clearly distinct from that seen with bilateral knockdown. Cavity formation was only delayed on the injected side (Fig. 9D), and the retarded cavity failed to reach its normal size while the contralateral cavity underwent excessive inflation (Fig. 10E). This asymmetry caused the germinal plate to curve sharply towards the injected side (Fig. 10F), but in contrast to bilateral injections the overinflated cavity did not indent the midgut primordium nor did the primordium lose its normal attachment to the germinal plate. After hatching, the curved embryos produced by unilateral *Pax3/7A* knockdown underwent relatively normal dorsal closure.

MO2 only produced asymmetric inflation of the dorsal body cavities if the M teloblast was injected early in its sequence of stem cell divisions. Relying on the 1:1 relationship of primary m blast cells to mature segments, we used the fluorescein-tagged MO as a lineage tracer to retroactively calculate the number of unlabeled blast cells that had been produced prior to teloblast injection. MO2 injection resulted in severely asymmetric body cavities in 95% (198/208) of embryos in which MO2 was injected after the M teloblast had produced 0–7 blast cells. In contrast, MO2 only produced a weak asymmetry when the teloblast was injected after producing 9–10 blast cells (8/9 embryos), and had no discernable effect on symmetry when the teloblast was injected after producing 12–30 blast cells ($n=132$ embryos).

The only mesoderm located at the site of dorsal cavity formation is a population of migratory mesenchymal cells situated between the provisional integument and the midgut primordium (Nelson and Weisblat, 1992). These cells do not express *Hau-Pax3/7A* during normal development. Nonetheless, we considered the possibility that knocking down gene expression in the precursor mesoderm might alter their development and thereby elicit the body cavity phenotype. However, following *Hau-Pax3/7A* knockdown in the ipsilateral M teloblast, these cells migrate appropriately (Fig. 11B) and differentiate into extraembryonic muscle fibers as in normal development.

On the other hand, *Hau-Pax3/7A* knockdown has a profound effect on the morphogenesis of the segmental mesoderm within the germinal plate. The germinal bands meet along the ventral midline to form the germinal plate (Fig. 1B). During normal development optical sectioning reveals that the m blast cell clones adopt a scalloped morphology of concave depressions on their medial surface (Fig. 11A), where they silhouette lateral bulges of the neuroectodermal N teloblast lineage (Shain et al., 1998). But when *Hau-Pax3/7A* is knocked down in the ipsilateral mesoderm, those m blast cell clones that receive the antisense MO adopt highly variable morphologies when they reach this same location (Fig. 11A). MO-treated clones fail to produce a regular pattern of medial concavities, and some extend abnormal projections into the overlying ectoderm of the germinal plate. These morphological abnormalities were seen on both sides of the germinal plate when antisense MOs were introduced

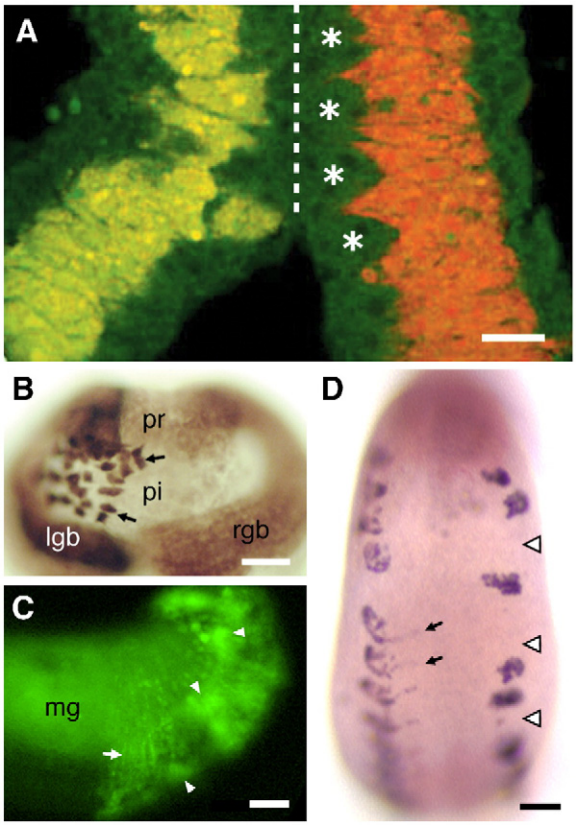

Fig. 11. Effects of *Hau-Pax3/7A* knockdown on mesoderm development. (A) Optical section of germinal bands fusing at the ventral midline (dashed line), with anterior towards the top. The mesoderm is labeled bilaterally with rhodamine–dextran, and left mesoderm is also labeled with fluorescein-tagged antisense MO. The m blast cell clones (red) in the right germinal band are developing normally, and form a pattern of segmentally repeated concavities encircling lateral bulges of neuroectoderm (asterisks), which can be seen by green autofluorescence. In contrast, the MO-treated blast cell clones (yellow) in the left germinal band adopt irregular morphologies where they enter the germinal plate. (B) *Hau-Pax3/7A* knockdown does not prevent M-derived mesenchyme from migrating into the provisional integument. In this late stage 7 embryo, the left mesoderm contains anti-*Hau-Pax3/7A* MO and biotin–dextran lineage tracer. Tracer staining (brown) is visible in the left germinal band (lgb) and migratory mesenchyme cells (arrows) underneath the unlabeled provisional integument (pi). The right germinal band (rgb) and prostomium (pr) show background staining. (C) Effect of *Hau-Pax3/7A* knockdown on mesoderm differentiation. Side view of stage 10 embryo with anterior to the left and dorsal to the top. The left M teloblast was injected with fluorescein-tagged antisense MO midway through blast cell production, and MO-containing tissues are visualized by fluorescence. The MO-treated mesoderm has given rise to normal derivatives such as circular muscle fibers (arrow), as well as irregular clumps of uncertain tissue type (arrowheads). The midgut (mg) yolk shows diffuse autofluorescence. (D) *Hau-Pax3/7A* knockdown interferes with nephridial development. Stage 10 embryo seen in ventral view with anterior to the top, and nephridia stained by *Hau-Pax3/7A in situ* hybridization. Arrows mark the ventral extensions of nephridia on the embryo's right. Mesoderm on the embryo's left side received antisense MO at stage 7. Arrowheads mark segments where nephridia are missing or greatly reduced. Those nephridia that did form have abnormal morphology and fail to extend tubules towards the ventral midline. Scale bars: 25 μm in panel A; 50 μm in panels B–D.

bilaterally, and were never observed following injection of control MOs.

The variable morphogenetic behavior of the m blast cell clones that receive MO2 disrupts the segmental organization of the germinal plate. Nonetheless, the mesoderm differentiates to produce many of its normal derivatives, which are intermingled with irregular clumps of M-derived tissue of uncertain histotype (Fig. 11C). Both circular and longitudinal muscles form within the body wall mesoderm, although their density is reduced. The antisense-treated mesoderm also contributes its normal descendants to the ventral nerve cord (Weisblat and Shankland, 1985), even though the neural tissue fails to form segmentally organized ganglia on that side (Fig. 12).

Development of the nephridia is particularly sensitive to mesodermal knockdown of *Hau-Pax3/7A*. We could not identify nephridia by morphological criteria alone in antisense-treated specimens, and therefore relied on *Hau-Pax3/7A* RNA as a molecular marker of nephridial differentiation. We injected MO2 into the left M teloblast of twelve stage 7 embryos, and sacrificed them at stage 10 for *in situ* hybridization. The *Helobdella* embryo normally produces 15 nephridia/side, and *in situ* hybridization revealed an average of 14.2 nephridia on the uninjected side and 6.3 nephridia on the MO2-treated side. Thus, *Hau-Pax3/7A* knockdown was sufficient to prevent the specification and/or molecular

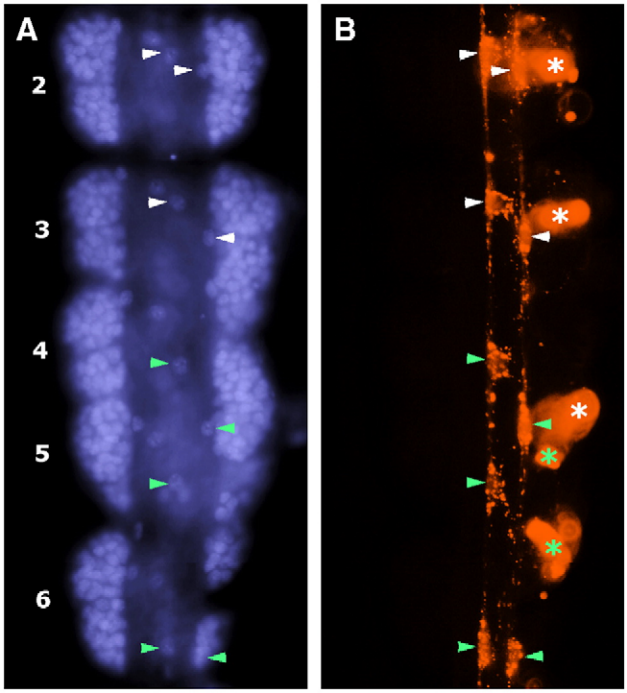

Fig. 12. Morphological disruption of nervous system segmentation following *Hau-Pax3/7A* knockdown in the mesoderm. Hoechst (A) and rhodamine (B) fluorescence images of dissected nerve cord from a stage 10 embryo. Midbody ganglia are numbered on the left. The right mesoderm contained antisense MO posterior to the third midbody segment. (A) The distribution of nuclei reveals the normal segmental pattern of ganglion formation on the left, but ganglion profiles are irregular and/or fused on the right. Arrowheads point to the nuclei of the connective muscle fibers marked in part B. (B) Rhodamine–dextran lineage tracer reveals the contribution of the right M teloblast to the ventral nerve cord, including spindle-shaped connective muscle fibers (arrowheads) and small clusters of neurons (asterisk). Cells that also contained the fluorescein-tagged antisense MO are marked with green symbols. Antisense MO does not prevent the differentiation of these mesodermal derivatives, even though the segmental organization of the ganglia is disrupted.

differentiation of nephridia in the majority of segments where that organ would normally form. Those nephridia that did develop from MO2-treated mesoderm were globular cell masses that lacked the normal tubular morphology and failed to extend ventrally towards the site of the excretory pore (Fig. 10D).

Discussion

Hau-Pax3/7A is one of a pair of Group III *Pax* genes from the leech *Helobdella* sp. (Austin), and the first member of this subfamily to be described in the superphylum *Lophotrochozoa*. Maternal expression of *Hau-Pax3/7A* is broadly distributed in the teloplasm, a cytoplasmic domain inherited by both mesodermal and ectodermal blastomeres. However, this early expression disappears around the onset of blast cell formation, and is replaced by what appears to be zygotic expression restricted to the blast cells of the mesodermal germ layer. MO knockdown experiments indicate that *Hau-Pax3/7A* plays critical roles in segmental morphogenesis, nephridial development, and body cavity formation.

Mesoderm differentiation

The newly born blast cells of the leech embryo experience an upsurge in zygotic transcription that has been likened to the midblastula transition of amphibian and fly embryos (Bissen and Weisblat, 1991). *Hau-Pax3/7A* is the first identified gene that has been shown to be part of this wave of zygotic expression. The m blast cells express *Hau-Pax3/7A* RNA within 1.5 h after their birth, and at stages when there is little or no detectable RNA to be inherited from the parent teloblast. However, expression of *Hau-Pax3/7A* is restricted to only one of the five teloblast lineages and therefore not a general feature of blast cell development *per se*. Early expression of *Hau-Pax3/7B* is similarly restricted to the blast cell progeny of the neuroectodermal N teloblast (M. Shankland, unpublished), suggesting that lineage-specific patterns of zygotic gene expression may play an important role in the developmental diversification of the teloblast lineages.

We examined the function of *Hau-Pax3/7A* in mesoderm development by injecting zygotes or identified blastomeres with antisense MOs targeted to the translation start site of the mRNA. Antisense MOs targeted to two different parts of the mRNA sequence gave the same developmental phenotypes, whereas parallel injections of two control MOs had little or no effect on development. Our antisense MOs only produced developmental abnormalities when introduced into the mesodermal cell lineages where this gene is normally expressed, suggesting that these particular MO sequences do not disrupt other, untargeted gene products that are involved in the development of multiple cell lineages.

During normal development the m blast cell clone changes shape as it enters the germinal plate, including the formation of a concave medial surface that encircles a lateral bulge in the neuroectoderm (Fig. 11A; compare to Shain et al., 1998). Those m blast cell clones that were subjected to *Hau-Pax3/7A* knockdown appeared relatively normal until they approached the germinal plate, but there adopted irregular and highly variable morphologies. Most of the antisense-treated clones failed to form a distinct medial concavity, and some made aberrant extensions into the overlying ectodermal cell layer. These morphological defects suggest that the Hau-Pax3/7A transcription factor may govern the expression of gene products involved in cell adhesion between germ layers, or regulators of cytoskeletal organization.

The variable morphogenetic behavior of the antisense-treated m blast cell clones disrupts the segmental periodicity of the germinal plate, a phenomenon that is reflected in later stages by disorganized patterns of segmental organogenesis. For example, antisense-treated mesoderm makes its normal contribution of neurons and muscle fibers to the central nervous system, but the coalescence of neurons into segmentally organized ganglia is severely disrupted on the treated side. A similar but more severe disruption of gangliogenesis is seen following unilateral ablation of the leech mesoderm (Blair, 1982; Torrence et al., 1989).

Hau-Pax3/7A expression is also critical for the development of one particular organ, the nephridium. In segments that generate nephridia, *Hau-Pax3/7A* expression occurs initially in the precursor cell or nephridioblast and later in the differentiating nephridial tissues. Mesodermal knockdown of *Hau-Pax3/7A* blocked the formation of nephridia in more than half of the treated segments, and those nephridia that did form in the presence of antisense MOs lacked their normal tubular morphology. Each individual m blast cell clone goes through multiple phases of *Hau-Pax3/7A* expression, and it may be that one or more of the early phases is required for the specification of the nephridioblast and one or more of the later phases for tubule morphogenesis.

Hau-Pax3/7A is also expressed transiently during the organogenesis of a previously undescribed mesodermal structure in four anterior segments that do not produce nephridia. These obliquely oriented bar-shaped structures lie in close proximity to the midgut primordium, and may be associated with gut development. However, their ultimate fate is unknown, and *Hau-Pax3/7A* knockdown did not produce any phenotypes that we could readily ascribe to their disruption.

Body cavity formation

The dorsal body cavities of the leech embryo arise during gastrulation when an extraembryonic membrane – the provisional integument – separates from the yolk-filled midgut primordium. These dorsal cavities are distinct from the coelom and lie outside the germinal plate (Nardelli-Haefliger and Shankland, 1993). During later development they are obliterated by dorsal closure of the body wall.

We have found that mesodermal knockdown of *Hau-Pax3/7A* selectively delays the separation of integument and midgut on the injected side(s), although the cellular basis of this phenomenon is unclear. There is a population of M-derived mesenchyme that migrates over the inner surface of the provisional integument (Nelson and Weisblat, 1992), and it is

possible that these migratory cells help to initiate cavity formation by some unknown mechanism that lies downstream of *Hau-Pax3/7A* expression. The migratory cells do not themselves express *Hau-Pax3/7A*, and *Hau-Pax3/7A* knockdown does not appear to alter their pattern of migration nor their later differentiation into provisional integument muscle fibers. Even so, it is possible that these cells play some role in initiating body cavity formation that is separate from their overt differentiation.

An alternative possibility is that the segmentally organized mesoderm within the germinal plate generates an extracellular signal that promotes the separation of provisional integument and midgut at a distance. Several lines of circumstantial evidence are consistent with this hypothesis. Separation of integument and midgut begins immediately adjacent to the sides of the anterior germinal plate (Fig. 9B). In addition, one should note that only the anteriormost (i.e., firstborn) m blast cells have reached the germinal plate (cf., Fig. 1) at the onset of dorsal cavity formation, and that a delay in separation was only observed if anti-*Pax3/7A* MO was introduced into the first 7–10 blast cells produced by the M teloblast.

Bilateral knockdown of *Hau-Pax3/7A* expression in the mesoderm not only delays the formation of the dorsal body cavities, it also results in their overinflation accompanied by a morphological collapse of the midgut primordium. Here again it is not clear how *Hau-Pax3/7A* expression in the mesoderm influences these events, or why only bilateral knockdown leads to midgut collapse. The principal defect is unlikely to be a reduction in mesoderm:midgut adhesion, since the collapsing midgut undergoes profound shrinkage before it begins to visibly detach from the germinal plate.

Inflation of the blastocoel and brain ventricles in vertebrate embryos is driven by directional ion transport coupled to osmosis (Watson and Barcroft, 2001; Lowery and Sive, 2005). By analogy, the body cavity overinflation seen here could be an indirect result of disrupted or unregulated transport. This might occur if the Hau-Pax3/7A transcription factor controls the expression of gene products involved in membrane transport, an idea that could explain why this gene has an impact on body cavity formation and is also expressed in the differentiated tissues of an excretory organ.

Maternal expression

The *Helobdella* embryo receives a large contribution of maternal *Hau-Pax3/7A* RNA, but the developmental function of the maternal transcripts remains to be determined. MO injection of either DM″ or the two M teloblasts yields phenotypes that are outwardly similar to those obtained with zygote injections. Thus, any role that *Hau-Pax3/7A* may play outside the mesoderm appears to be obscured in zygote injections by the severe phenotypes deriving from knockdown in the mesoderm. Some of those mesodermal phenotypes may depend upon an abrogation of maternal *Hau-Pax3/7A* expression, but it is difficult to draw that distinction given that the mesodermal cell lineage also experiences widespread zygotic expression.

In an attempt to circumvent the phenotypes produced by knockdown of *Hau-Pax3/7A* in the mesoderm, we injected the antisense MO into ectodermal progenitor cell DNOPQ‴. This blastomere inherits a substantial fraction of the *Hau-Pax3/7A* transcripts present in the zygote's teloplasm (Fig. 5B), but the antisense MO had no discernable effect on the development of its descendants. This result may indicate that maternal transcripts play no role in ectoderm development, but it is also possible that the maternal *Hau-Pax3/7A* RNA had already been used for protein synthesis before the stage when antisense MOs were injected.

Evolution of the Pax III subfamily

Hau-Pax3/7A and *-Pax3/7B* are the first *Pax III* genes reported from the superphylum *Lophotrochozoa*, and as such shed new light on the evolutionary history of this subfamily of genes. The *Pax III* genes play extensive roles in neural patterning and neurogenesis in both deuterostomes and ecysozoans (Mansouri et al., 1996; Wada et al., 1997; Holland et al., 1999; Davis et al., 2005), which has been taken as evidence that an ancestral *Pax III* gene was most likely involved in the neural development of early bilaterian animals. Consistent with this view, the leech's *Hau-Pax3/7B* gene is primarily expressed in the developing blast cells of the neuroectodermal N teloblast lineage (M. Shankland, unpublished).

In contrast, there is no detectable expression of *Hau-Pax3/7A* in the leech nervous system, and only very limited expression in the prostomial ectoderm. It seems very likely that these two leech *Pax III* genes arose through duplication of an ancestral gene, and one possibility is that the ancestral gene had dual roles in mesodermal and neural development. Thus, the two paralogs could have subdivided the ancestral functions, with each gene inheriting only those developmental functions associated with a particular germ layer. However, at the present time we cannot rule out an alternative scenario in which the expression of *Hau-Pax3/7A* was displaced from neuroectoderm to mesoderm following its separation from *Hau-Pax3/7B*. A *Pax III* gene has recently been isolated from the polychaete annelid *Capitella* (E.C. Seaver, personal communication), and its characterization may help to distinguish between these possibilities.

Prior to this study, extensive mesodermal expression of *Pax III* genes has not been reported outside of chordates. Indeed, the absence of mesodermal expression in urochordate larvae led Kusakube and Kuratani (2005) to propose that broad mesodermal expression of Pax III is a recent acquisition within the chordate radiation. The latter conclusion must be revisited given the phylogenetic analysis of Blair and Hedges (2005), which indicates that cephalochordates – which, like vertebrates, express their *Pax III* gene in somitic mesoderm (Holland et al., 1999) – are the basal branch of the chordate radiation. In addition, our present findings show that a *Pax III* gene is broadly expressed in the developing mesoderm of a lophotrochozoan embryo. These data are consistent with two alternative evolutionary histories. One possibility is that broad mesodermal expression of *Pax III* genes is a derived trait that

evolved independently in the lineages that gave rise to chordates and leeches. But one must also consider a scenario in which the *Pax III* gene(s) showed broad mesodermal expression in the last common ancestor of the bilaterian superphyla, and that mesodermal expression was independently lost, or greatly reduced, in lineages that gave rise to arthropods and to urochordates. *Pax III* genes will need to be characterized in a wider diversity of taxa before these alternatives can be resolved with any certainty.

Like many other lophotrochozoans, the leech embryo undergoes spiral cleavage and produces a single blastomere – the mesentoblast – that generates most of the mesoderm in its adult body plan. There is a rich embryological literature on the developmental events that lead to mesentoblast specification, which relies on cell-intrinsic and -extrinsic factors to varying degrees in different taxa (Freeman and Lundelius, 1992; van den Biggelaar et al., 1997). The activation of the MAP kinase ERK in the mesentoblast and/or its parent blastomere seems to be a critical step in all spiralians examined (Lambert and Nagy, 2003). ERK activation brings about a precocious expression of *Brachyury* (*Bra*) in the mesentoblast lineage of the limpet *Patella* (Lartillot et al., 2002), although *Bra* is expressed in surrounding tissues as well.

In leech, *Hau-Pax3/7A* is expressed by the m blast cells and is therefore an early marker for essentially the entire mesodermal germ layer. There are no previous reports of *Pax III* gene expression in spiralians or other lophotrochozoans, so it is not clear how widely this phenomenon is conserved. A few other spiralian genes are also known to be expressed during mesoderm differentiation (Yang and Collier, 1993; Le Gouar et al., 2003). In particular, Hinman and Degnan (2002) found that the *Meox* gene (also called '*Mox*') is selectively expressed in the mesodermal bands of the trochophore larva in the abalone *Haliotis*. This observation is intriguing given that Pax3 and Meox proteins of vertebrates physically interact (Stamataki et al., 2001), and both play important roles in somite development (Mankoo et al., 2003). Further work will be needed to learn whether these two gene families also interact during the mesoderm differentiation of spiralians such as the leech.

Acknowledgments

Authors would like to thank John Wallingford for his confocal microscope and Greg Davis and Nipam Patel for guiding us into the study of *Pax III* genes. Work was supported by NSF grant IBN-0415732 and funds from the U. Texas Austin Vice President of Research.

References

Balczarek, K.A., Lai, Z.-C., Kumar, S., 1997. Evolution and functional diversification of the Paired Box (Pax) DNA-binding domains. Mol. Biol. Evol. 14, 829–842.

Bely, A.E., Weisblat, D.A., 2006. Lessons from leeches: a call for DNA barcoding in the lab. Evol. Dev. 8, 491–501.

Bissen, S.T., Weisblat, D.A., 1989. The durations and compositions of cell cycles in embryos of the leech, *Helobdella triserialis*. Development 105, 105–118.

Bissen, S.T., Weisblat, D.A., 1991. Transcription in leech: mRNA synthesis is required for early cleavages in *Helobdella embryos*. Dev. Biol. 146, 12–23.

Blair, S.S., 1982. Interactions between mesoderm and ectoderm in segment formation in the embryo of a glossiphoniid leech. Dev. Biol. 89, 389–396.

Blair, J.E., Hedges, S.B., 2005. Molecular phylogeny and divergence times of deuterostome animals. Mol. Biol. Evol. 22, 2275–2284.

Boyer, B.C., Henry, J.J., Martindale, M.Q., 1998. The cell lineage of a polyclad turbellarian embryo reveals close similarity to coelomate spiralians. Dev. Biol. 204, 111–123.

Bürger, O., 1891. Beiträge zur Entwicklungsgeschichte der Hirudineen. Zur Embryologie von Nephelis. Zool. Jb. anat. 4, 697–783.

Davis, G.K., Jaramillo, C.A., Patel, N.H., 2001. *Pax* group III genes and the evolution of insect pair-rule patterning. Development 128, 3445–3458.

Davis, G.K., D'Alessio, J.A., Patel, N.H., 2005. *Pax3/7* genes reveal conservation and divergence in the arthropod segmentation heirarchy. Dev. Biol. 285, 169–184.

Dearden, P.K., Donly, C., Grbic, M., 2002. Expression of pair-rule gene homologues in a chelicerate: early patterning of the two-spotted spider mite *Tetranychus urticae*. Development 129, 5461–5472.

Freeman, G., Lundelius, J.W., 1992. Evolutionary implications of the mode of D-quadrant specification in coelomates with spiral cleavage. J. Evol. Biol. 5, 205–247.

Goldstein, B., Leviten, M.W., Weisblat, D.A., 2001. Dorsal and Snail homologs in leech development. Dev. Genes Evol. 211, 329–337.

Goulding, M.D., Chalepakis, G., Deutsch, U., Erselium, J.R., Gruss, P., 1991. Pax-3, a novel murine DNA binding protein expressed during early neurogenesis. EMBO J. 10, 1135–1147.

Goulding, M.D., Lumsden, A., Paquette, A.J., 1994. Regulation of Pax-3 expression in the dermomyotome and its role in muscle development. Development 120, 957–971.

Gutjahr, T., Patel, N.H., Li, X., Goodman, C.S., Noll, M., 1993. Analysis of the *gooseberry* locus in *Drosophila* embryos: *gooseberry* determines the cuticular pattern and activates *gooseberry neuro*. Development 118, 21–31.

Henry, J.Q., Martindale, M.Q., 1998. Conservation of the spiralian developmental program: cell lineage of the nemertean, *Cerebratulus lacteus*. Dev. Biol. 201, 253–269.

Hinman, V.F., Degnan, B.M., 2002. Mox homeobox expression in muscle lineage of the gastropod *Haliotis asinina*: evidence for a conserved role in bilaterian myogenesis. Dev. Genes Evol. 212, 141–144.

Hobert, O., Ruvkun, G., 1999. *Pax* genes in *Caenorhabditis elegans*: a new twist. Trends Genet. 15, 214–216.

Holland, L.Z., Schubert, M., Kozmik, Z., Holland, N.D., 1999. *AmphiPax3/7*, an amphioxus paired box gene: insights into chordate myogenesis, neurogenesis, and the possible evolutionary precursor of definitive vertebrate neural crest. Evol. Dev. 1, 153–165.

Holton, B., Wedeen, C.J., Astrow, S.H., Weisblat, D.A., 1994. Localization of polyadenylated RNAs during teloplasm formation and cleavage in leech embryos. Roux's Arch. Dev. Biol. 204, 46–53.

Kusakube, R., Kuratani, S., 2005. Evolution and developmental patterning of the vertebrate skeletal muscles: perspectives from the lamprey. Dev. Dyn. 234, 824–834.

Lambert, J.D., Nagy, L.M., 2003. The MAPK cascade in equally cleaving spiralian embryos. Dev. Biol. 263, 231–241.

Lartillot, N., Lespinet, O., Vervort, M., Adoutte, A., 2002. Expression pattern of Brachyury in the mollusc Patella vulgata suggests a conserved role in the establishment of the AP axis in Bilateria. Development 129, 1411–1421.

Le Gouar, M., Lartillot, N., Adoutte, A., Vervoort, M., 2003. The expression of a caudal homologue in a mollusc, Patella vulgata. Gene Express. Pattern 3, 35–37.

Lowery, L.A., Sive, H., 2005. Initial formation of zebrafish brain ventricles occur independently of circulation and requires the *nagie oko* and *snakehead/atp1a1a.1* gene products. Development 132, 2057–2067.

Mankoo, B.S., Skuntz, S., Harrigan, I., Grigorieva, E., Candia, A., Wright, C.V. E., Arnheiter, H., Pachnis, V., 2003. The concerted action of *Meox* homeobox genes is required upstream of genetic pathways essential for the formation, patterning, and differentiation of somites. Development 130, 4664–4855.

Mansouri, A., Stoykova, A., Torres, M., Gruss, P., 1996. Dysgenesis of cephalic neural crest derivatives in *Pax7−/−* mutant mice. Development 122, 831–838.

Matus, D.Q., Pang, K., Daly, M., Martindale, M.Q., 2007. Expression of *Pax* gene family members in the anthozoan cnidarian, *Nematostella vectensis*. Evol. Dev. 9, 25–38.

Mazet, F., Hutt, J.A., Millard, J., Shimeld, S.M., 2003. *Pax* gene expression in the developing central nervous system of *Ciona intestinalis*. Gene Expr. Patterns 3, 743–745.

Miller, D.J., Hayward, D.C., Reece-Hoyes, J.S., Scholten, I., Catmull, J., Gehring, W.J., Callaerts, P., Larsen, J.E., Ball, E.E., 2000. *Pax* gene diversity in the basal cnidarian *Acropora millepora* (Cnidaria, Anthozoa): implications for the evolution of the *Pax* gene family. Proc. Natl. Acad. Sci. U. S. A. 97, 4475–4480.

Nardelli-Haefliger, D., Shankland, M., 1992. *Lox2*, a putative leech segment identity gene, is expressed in the same segmental domain in different stem cell lineages. Development 116, 697–710.

Nardelli-Haefliger, D., Shankland, M., 1993. *Lox10*, a member of the *NK-2* homeobox gene class, is expressed in a segmental pattern in the endoderm and in the cephalic nervous system of the leech *Helobdella*. Development 118, 877–892.

Nelson, B.H., Weisblat, D.A., 1992. Cytoplasmic and cortical determinants interact to specify ectoderm and mesoderm in the leech embryo. Development 115, 103–115.

Noll, M., 1993. Evolution and role of *Pax* genes. Curr. Opin. Genet. Dev. 3, 595–605.

Oustanina, S., Hause, G., Braun, T., 2004. Pax7 directs postnatal renewal and propagation of myogenic satellite cells but not their specification. EMBO J. 23, 3430–3439.

Passamaneck, Y., Halanych, K.M., 2006. Lophotrochozoan phylogeny assessed with LSU and SSU data: evidence of lophophorate polyphyly. Mol. Phyl. Evol. 40, 20–28.

Rivera, A.J., Gonsalves, F.C., Song, M.H., Norris, B.J., Weisblat, D.A., 2005. Characterization of Notch-class gene expression in segmentation stem cells and segment founder cells in *Helobdella robusta* (*Lophotrochozoa*; *Annelida*; *Clitellata*; *Hirudinida*; *Glossiphoniidae*). Evol. Dev. 7, 588–599.

Schoppmeier, M., Damen, W.G.M., 2005. Expression of *Pax* group III genes suggests a single-segmental periodicity for opisthosomal segment patterning in the spider *Cupiennius salei*. Evol. Dev. 7, 160–169.

Seaver, E.C., Shankland, M., 2000. Leech segmental repeats develop normally in the absence of signals from either anterior or posterior segments. Dev. Biol. 224, 339–353.

Shain, D., Ramirez-Weber, F.A., Hsu, J., Weisblat, D.A., 1998. Gangliogenesis in leech: morphogenetic processes leading to segmentation in the central nervous system. Dev. Genes Evol. 208, 28–36.

Shankland, M., Weisblat, D.A., 1984. Stepwise commitment of blast cell fates during the positional specification of the O and P cell lines of the leech embryo. Dev. Biol. 106, 326–342.

Smith, C.M., Weisblat, D.A., 1994. Micromere fate maps in leech embryos: lineage-specific differences in rates of cell proliferation. Development 120, 3427–3438.

Song, M.H., Huang, F.Z., Chang, G.Y., Weisblat, D.A., 2002. Expression and function of an even-skipped homolog in the leech *Helobdella robusta*. Development 129, 3681–3692.

Song, M.H., Huang, F.Z., Gonsalves, F.C., Weisblat, D.A., 2004. Cell cycle-dependent expression of a *hairy and Enhancer of split* (*hes*) homolog during cleavage and segmentation in leech embryos. Dev. Biol. 269, 183–195.

Stamataki, D., Kastrinaki, M.C., Mankoo, B.S., Pachnis, V., Karagogeos, D., 2001. Homeodomain proteins Mox1 and Mox2 associate with Pax1 and Pax3 transcription factors. FEBS Lett. 499, 274–278.

Stent, G.S., Kristan Jr., W.B., Torrence, S.A., French, K.A., Weisblat, D.A., 1992. Development of the leech nervous system. Int. Rev. Neurobiol. 33, 109–133.

Torrence, S.A., Law, M.I., Stuart, D.K., 1989. Leech neurogenesis: II. Mesodermal control of neural patterns. Dev. Biol. 136, 40–60.

van den Biggelaar, J.A.M., Dictus, W.J.A.G., van Loon, A.E., 1997. Cleavage patterns, cell-lineages, and cell specification are clues to phyletic lineages in Spiralia. Semin. Cell Dev. Biol. 8, 367–378.

Wada, H., Holland, P.W.H., Sato, S., Yamamoto, H., Satoh, N., 1997. Neural tube is partially dorsalized by overexpression of *HrPax-37*: the ascidian homologue of *Pax-3* and *Pax-7*. Dev. Biol. 187, 240–252.

Watson, A.J., Barcroft, L.D., 2001. Regulation of blastocyst formation. Front. Biosci. 6, D708–D730.

Weisblat, D.A., Shankland, M., 1985. Cell lineage and segmentation in the leech. Philos. Trans. R. Soc. Lond., B 312, 39–56.

Yang, K., Collier, J.R., 1993. Localized expression of the H-ras proto-oncogene during *Ilyanassa* development. Dev. Biol. 157, 303–307.

Zackson, S.L., 1982. Cell clones and segmentation in leech development. Cell 31, 761–770.

Zackson, S.L., 1984. Cell lineage, cell–cell interaction, and segment formation in the ectoderm of a glossiphoniid leech embryo. Dev. Biol. 104, 143–160.